Journal of Environmental Protection, 2025, 16(10), 1066-1081
https://www.scirp.org/journal/jep
ISSN Online: 2152-2219
ISSN Print: 2152-2197

Computational Fluid Dynamics Modeling to Facilitate Qualification of Stack Sampling Probe Location

Sarah R. Suffield[1*], John Matthew Barnett[1,2], Julia E. Flaherty[1]

[1]Pacific Northwest National Laboratory, Richland, Washington, USA
[2]Washington State Department of Health, Radioactive Air Emissions Section, Richland, Washington, USA
Email: *sarah.suffield@pnnl.gov

How to cite this paper: Suffield, S.R., Barnett, J.M. and Flaherty, J.E. (2025) Computational Fluid Dynamics Modeling to Facilitate Qualification of Stack Sampling Probe Location. *Journal of Environmental Protection*, **16**, 1066-1081.
https://doi.org/10.4236/jep.2025.1610057

Received: September 18, 2025
Accepted: October 26, 2025
Published: October 29, 2025

Abstract

Computational fluid dynamics (CFD) modeling was used to help evaluate modifications to a radiological effluent stack and assist with establishing a stack sampling location that met the mixing criteria for qualification. Requirements for stack sampling location are listed in the American National Standards Institute/Health Physics Society (ANSI/HPS) N13.1-2021 standard. Modeling was performed to help develop a suitable design for increasing building ventilation for the radiological effluent stack. The ANSI/HPS N13.1-2021 criteria for the air monitoring probe location are that the coefficient of variation of velocity uniformity, gaseous tracer uniformity, and particulate tracer uniformity must be less than or equal to 20%. Furthermore, no point in the sampling location may have a gaseous tracer concentration that varies from the mean concentration by more than 30%. Additionally, the flow angle at the sampling location must not be more than 20 degrees. The ANSI/HPS N13.1-2021 standard allows for models (physical or computational) to be employed to perform the full suite of qualification tests, followed by a more limited set of verification tests on the actual stack to qualify the stack sampling location. Here, a series of computational model simulations were employed to evaluate the stack qualification criteria. Significant time and resource savings are achieved using CFD modeling. CFD modeling demonstrated that the stack meets the criteria at the sample probe location. Verification tests were performed on the modified stack to measure the velocity uniformity and flow angle at the stack sampling location, and results demonstrated that the CFD model results may be used to support the qualification of the stack sampling location.

Keywords

Atmospheric Emissions, Air Monitoring, Environmental Monitoring, Compuatational Modeling, Standards

1. Introduction

The 3430 Building at Pacific Northwest National Laboratory houses radiological capabilities. Because the building is a U.S. Department of Energy facility, permit conditions require that air discharged from the building filtered exhaust stack system be monitored for radionuclides. The air monitoring system requires a sampling probe in the exhaust stream that conforms to the uniformity criteria of the American National Standards Institute/Health Physics Society (ANSI/HPS) N13.1-2021 standard [1][1]. The criteria at the stack sampling location are as follows:

- The average angle between the flow and duct axis must be less than 20 degrees.
- The uniformity of flow velocity must have a coefficient of variation (COV) of less than or equal to 20%.
- The uniformity of tracer gas must have a COV of less than or equal to 20%.
- No point in the sampling plane should have a tracer gas concentration that exceeds the mean by more than 30%.
- The uniformity of tracer particles must have a COV of less than or equal to 20%.

The COV is defined as the standard deviation divided by the mean, reported as a percentage.

The ANSI/HPS N13.1-2021 standard allows adoption of results from a previously performed full test series for a stack system of similar configuration as the basis of compliance with the standard. Compliance then is confirmed by partial, or verification, testing performed on the actual stack system. This approach was used to qualify the location of the monitoring probe and configuration of the original two-fan 3430 Building filtered exhaust stack as documented by Glissmeyer and Flaherty [2]. The verification testing performed on the actual system included flow angle and velocity uniformity measurements. The previous full test series applied as the basis for compliance was performed on a scale model of the HV-C2 air exhaust stack by Glissmeyer and Droppo [3]. The HV-C2 stack, which is located at a nearby facility, included two fans entering a horizontal main duct, both at 45-degree angles, in a manner similar to the original configuration of the 3430 Building exhaust stack.

The original testing of the HV-C2 scale model was performed to establish the sampling probe location for the actual HV-C2 stack [3]. The scale model showed small flow angles and high velocity uniformity. However, tracer gas/particle test COV values were greater than 20% at all but the test port furthest downstream.

[1]The regulatory cited version of the standard is ANSI/HPS N13.1-1999. It was reissued, essentially unchanged, in 2011. The 2021 standard is the current revision, which is referenced herein.

This is expected because a substantial length of duct is required to achieve the fully developed flow needed to provide mixing energy. For turbulent flow, this flow development length is considered to be roughly independent of the Reynolds number and is at least 10-duct diameters of length from the last disturbance [4][2]. The furthest test port on the HV-C2 scale model is similar in scaled distance to that of the 3430 Building sampling location. Thus, it is reasonable to expect that all of the main duct length of the 3430 Building exhaust system will be needed to provide sufficient mixing of gas and particles in the duct.

The average overall flow rate for the 3430 Building exhaust stack system with two fans was 16.75 m^3/s (35,500 cfm) for a 5-year period and as high as about 17.70 m^3/s (37,500 cfm) for a single year within that period [5]. The exhaust system was subsequently redesigned for additional ventilation capacity within the building and incorporated a third fan and associated ductwork to integrate the new fan into the stack. The original stack was demolished, and a larger-diameter stack was constructed that considered both the upstream and downstream distances in relation to the sampling location. The stack configuration was changed substantially relative to the previous stack. The new operating conditions allowed nominal operations over the range of 10.76 to 30.39 m^3/s (22,800 to 64,400 cfm) [6].

Computational fluid dynamics (CFD) modeling was used to help determine the final design of the new ventilation system to gain more insight into the expected performance of the modified stack and sampling location. ANSI/HPS N13.1-2021 discusses CFD modeling as an option for optimizing and upgrading an existing system and indicates the same requirements for qualifying the sample extraction system must be met (*i.e.*, verification tests following complete evaluation with a similar exhaust system or a scale model system) [1]. The final modeled design for the 3430 Building stack with three fans included an oversize air blender to improve gas and particle mixing.

Significant time and resource savings are achieved using CFD modeling compared with physical modeling [7]-[10]. The physical scale modeling process to develop and test a stack configuration involves converting design drawings to an appropriate scale version of the stack so that it may be constructed on a smaller footprint, followed by the actual construction of the scaled stack. When the stack construction is completed, tests are executed with calibrated instrumentation that includes pitot tubes, digital manometers, thermocouples, gas analyzers, mass flow controllers, and particulate counters. The gaseous tracers that have been used for the tests, sulfur hexafluoride or nitrous oxide, are greenhouses gases. While establishing a computational model and running simulations also can take significant time and energy, it can be achieved in a matter of weeks rather than the months necessary to establish a physical model. The computational model approach also

[2]These distances are also consistent with the original ANSI N13.1-1969 standard, which states the sampling point should be a minimum of five diameters downstream from abrupt changes in flow direction or prominent transitions [17].

eliminates the need to use greenhouse gases and tracer particles.

2. Modeling Methodology

A CFD model of the 3430 Building stack system was constructed to simulate the stack flow, including distributions of gas and particle tracers, to help determine if the modified system would satisfy the ANSI/HPS N13.1-2021 standard. Providing accurate predictions of flow angle, velocity, tracer gas, and tracer particle distributions (at the sampling location) requires an accurate prediction of the turbulent air flow with transport and mixing of the tracer species within it. The geometry and flow field of the exhaust stack system is complex and highly three-dimensional (3-D). Therefore, a representative boundary-fitted, 3-D flow model was developed with the commercially available CFD software, STAR–CCM+ (Siemens PLM Software, STAR-CCM+ 17.06, Plano Texas) [11].

Past CFD modeling of exhaust stacks has been shown to be useful in the design process and has been an effective predictor of flow angles and velocity and tracer COVs [8]-[10] [12]-[14]. The stack sampling methodology assumes isothermal conditions exist within the stack (*i.e.*, the flow is at ambient conditions with no temperature gradients); therefore, that assumption was adopted in the flow model. For isothermal flow solutions, STAR-CCM+ solves the Navier-Stokes conservation of mass and momentum equations, which for steady-state compressible and incompressible fluid flows are:

$$\frac{\partial}{\partial x_j}\left(\rho u_j\right)=0\,, \tag{1}$$

$$\frac{\partial}{\partial x_j}\left(\rho u_j u_i-\tau_{ij}\right)=-\frac{\partial p}{\partial x_i} \tag{2}$$

where the terms u_i and u_j represent absolute fluid velocity components in coordinate directions x_i ($i = 1, 2, 3$) and x_j ($j = 1, 2, 3$), ρ is the density, p is the pressure, and τ_{ij} is the fluid stress tensor, which for turbulent flows is represented by:

$$\tau_{ij}=2\mu\sigma_{ij}-\frac{2}{3}\mu\frac{\partial u_k}{\partial x_k}\delta_{ij}-\overline{\rho u_i' u_j'} \tag{3}$$

where μ is the dynamic viscosity, σ_{ij} is the rate of strain tensor, δ_{ij} is the Kronecker delta, u_i' and u_j' are fluctuations about the average velocity, and the overbar indicates the averaging of the fluctuations. The right-most term in Equation (3) represents the additional Reynolds stresses due to turbulent motion. These stresses are linked to the mean velocity via the turbulence model being used. In the simulations for this work, the generation and dissipation of turbulence is accounted for using a standard κ-ε turbulence model, which is a widely tested and validated two-equation closure model for the Reynolds average Navier-Stokes equations, as described in the STAR-CMM+ User Guide [11]. In past work by Recknagle *et al.* [9], a turbulence model comparison found the Reynolds average Navier-Stokes κ-ε model to be the most suitable for simulating duct flow, a finding corroborated by Jensen [15]. To capture strong secondary flows, which are fre-

quently seen in heating, ventilation, and air conditioning (HVAC) systems, nonlinear terms were added to the stress-strain relationship for the κ-ε model by selecting a cubic constitutive relationship. This modified the Boussinesq approximation with cubic terms [11].

For the tracer gas simulations, the model assumes each species k of a gas mixture, with local mass fraction Y_k, is governed by a species conservation equation of the form:

$$\frac{\partial}{\partial x_j}\left(\rho u_j Y_k + F_{k,j}\right) = S_k, \tag{4}$$

where $F_{k,j}$ is the gas diffusional flux component and S_k is the gas species source term, which is non-zero at the injection location.

A Lagrangian dispersed two-phase flow model is used for the particle transport simulations. The Lagrangian methodology considers the interactions of mass, momentum, and energy between the continuum and dispersed phase. In general, motion of the dispersed phase is influenced by that of the continuous phase and vice versa. The strength of the phase interactions depends on concentration, size, and density of the dispersed particle. For the present work, particle concentrations are small, as is the nominal particle size. Thus, momentum transfer from particles to air is negligibly small. In the model, the momentum equation for a particle, given by Newton's second law, is:

$$m_d \frac{\mathrm{d}u_d}{\mathrm{d}t} = F_{dr} + F_p + F_b \tag{5}$$

where m_d and u_d are the mass and velocity of the dispersed particle phase, F_{dr} is the drag force, F_p the pressure force, and F_b is body forces, including effect of the gravity and angular velocity vectors. Surface vapor pressure and mass transfer between phases are not considered here. The problem is considered isothermal and does not involve electrically charged flow; therefore, thermophoresis and electrostatic effects are not included. Because of the low concentration of the particles, separation and coalescence models were not considered.

2.1. Model Geometry and Computational Mesh

The 3-D geometry for the CFD model was generated using the commercial computer-aided design (CAD) software SolidWorks (Dassault Systems SolidWorks Corp., SolidWorks Premium 2021, Waltham, Massachusetts) based on design drawings. **Figure 1** shows the model geometry for the updated ventilation system for the 3430 Building with three-fans and an air blender. Air flow upstream and through the fans is not included in the model domain but is accounted for as turbulence added at each fan duct. Thus, the model domain includes the ductwork from just downstream of the fans to the stack exit. Each of the three fan outlet ducts has a cross-sectional area of 0.41 m^2 (1645 in^2). The geometry also includes the dampers just downstream of the fans. The dampers are in an open configuration. Typical tracer injection locations are mid-duct, just downstream of the fans,

and near the junction where all three fan streams converge. The sampling point is located 22.10 m (72.5 feet) downstream of the junction between the duct from Fan 2 and the main duct, or 15 diameters for the duct with a 1.47 m (58-inch) diameter.

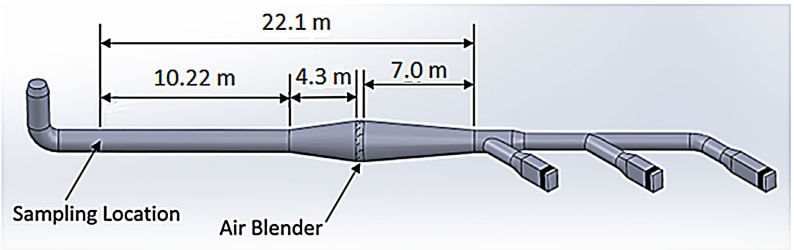

Figure 1. CAD geometry of 3430 Building exhaust system with the additional fan and static air blender.

A mesh sensitivity study was performed to ensure that the mesh was sufficiently resolved for the CFD model. The mesh sensitivity runs assumed only the fan closest to the sampling location was running at a total flowrate of 5.38 m^3/s (11,400 cfm). Three different resolutions of mesh were generated. An estimate of discretization error can be obtained by determining the Grid Convergence Index (GCI). This parameter is calculated following the approach outlined by Oberkampf and Roy [16]. The GCI is given by:

$$\mathrm{GCI} = \frac{F_s}{r^p - 1}\frac{\left|f_2 - f_1\right|}{f_1}, \tag{6}$$

where F_s is the factor of safety (equal to 1.25 for this calculation), r is the effective grid refinement factor, p is the order (which is 2 for these cases), and f_i is the solution for the cases, with f_1 designating the fine mesh solution and f_2 the solution for the coarse mesh. The effective grid refinement ratio can be computed as:

$$r = \left(\frac{N_1}{N_2}\right)^{1/D}, \tag{7}$$

where N_1 and N_2 are the total cell count for the fine and course meshes, respectively, and D is the dimensionality of the system. Applying this for the cell counts of the different mesh resolutions and resulting velocity uniformity in the CFD model shown in **Table 1** yields the two estimates of GCI, as shown in **Table 1**. Note that the GCI is not a bounding error estimate but rather is an indication of the relative error. The relative error for the coarse mesh was around 15% and the refined mesh was around 3%. The refined mesh is used going forward for the CFD model. **Figure 2(a)** provides a view of the mesh near Fan 2. The typical resolution throughout the volume mesh is represented in **Figure 2(b)**.

2.2. Boundary Conditions

Mass inflow boundaries were established at the duct inlets with turbulence intensity and length scale settings to account for upstream turbulence. The model

Table 1. GCI-CFD model.

Model	# Cells	Velocity Uniformity	GCI	Relative Error (%)
Coarse	509,136	3.0	0.0510	15
Refined	2,061,841	3.7	0.0088	3
Very Refined	6,143,642	3.6	N/A	N/A

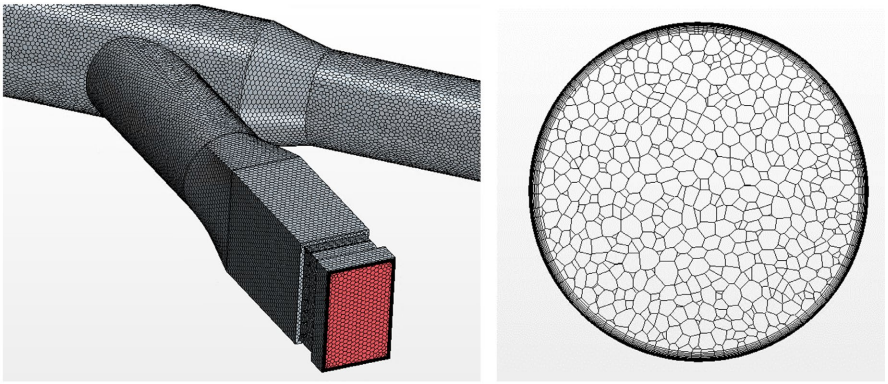

(a) (b)

Figure 2. Detail of computational mesh at the (a) surface near Fan 2, and (b) typical cross-section of the volume mesh in the main duct.

assumes a turbulent intensity value of 0.1 and a turbulent viscosity ratio of 100 at the model inlets. The turbulent viscosity ratio specifies the ratio of turbulent to laminar viscosity. A pressure boundary with 101 kPa (1 atmosphere) absolute pressure was used at the stack exit. Duct walls were modeled as smooth surfaces with zero slip flow boundary conditions. The particle boundary condition at the walls was established so particles with trajectories that impact the duct walls would stick to the surface.

2.2. Stack Model Benchmarking

The simulation cases presented in this section demonstrate the capability of the described CFD modeling methodology to suitably characterize the flow and sampling performance of an effluent stack. The methodology is validated by simulations that provide similar results to flow angle, velocity uniformity, gas tracer, and particle tracer data taken from actual stack performance testing.

The original 3430 Building two-fan stack was tested for flow angle and velocity uniformity [2]. Results for tracer gas and tracer particle sampling efficiency were inferred from data collected during previous tests [3] to determine if the stack meets the qualification criteria given in the standard. The inferred testing data were collected from a scaled physical model of the proposed design for the Hanford Waste Treatment and Immobilization Plant HV-C2 air exhaust stack, which is geometrically similar to the 3430 Building stack.

A 3-D CFD model of the original 3430 Building two-fan stack was created and

set up to replicate the geometry and flow conditions tested, and the 3430 Building original two-fan system is a similar configuration to the HV-C2 test model. Figure 3 is a photograph of the assembled HV-C2 physical test model showing the locations of Fans A and B (and their injection ports) and Test Ports 1, 2, and 3 along the main duct. Figure 4 shows the geometry and computational domain of the associated 3-D CFD model of the original 3430 two-fan system. The CFD model domain included the full duct from immediately downstream of the fans to the duct exit, and with mesh resolution similar to that discussed in the previous section.

Figure 3. HV-C2 physical test model.

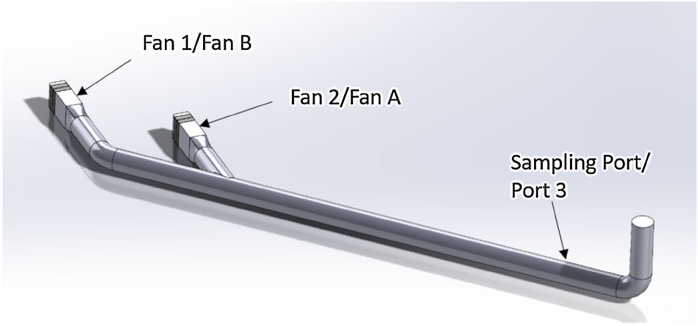

Figure 4. 3430 Building stack original two-fan system—3-dimensional CFD model.

Stack testing of the original 3430 Building two-fan system included velocity and flow angle measurements, which were used to benchmark the CFD model. Physical stack testing of the HV-C2 system included the flow angle, velocity uniformity, gas tracers, and particle tracer data for operations of one or two fans with various data collected at Test Ports 1, 2, and 3. The original 3430 Building system matches the testing results of the HV-C2 system most closely at Test Port 3. As such, gas and particle tracer data collected there were of interest when checking the results obtained from model benchmarking runs.

Table 2 through Table 5 summarize the CFD modeling benchmark/testing data comparisons. Table 2 compares velocity uniformity measured in testing of the original 3430 Building stack and predicted by the model. Table 3 shows the flow angle comparisons with the measured testing of the 3430 Building system. Table 4 and Table 5 show gas-tracer uniformity and particle-tracer uniformity comparisons

Table 2. Velocity uniformity comparison of measured data from 3430 tests (adapted from Table 4.2 of Glissmeyer and Flaherty [2]) and CFD results.

Fan Operating Configuration	Run Nr.	Measured Airflow (m^3/s)[a]	Measured COV	% CFD Model COV	%
Maximum (2 Fans, Sashes Open)	VT-4	16.10	3.8	3.3	
Maximum (2 Fans, Sashes Open)	VT-5	16.16	3.8		
Minimum (2 Fans, Sashes Closed)	VT-6	11.49	3.2	3.2	
Minimum (1 Fan, Sashes Closed)	VT-7	11.48	2.6	6.4	

[a]Original data in acfm = actual cubic feet per minute; to convert 1 m^3/s = 2118.88 cfm.

Table 3. Flow angle comparison of measured data from 3430 tests (adapted from Table 4.3 of Glissmeyer and Flaherty [2]) and CFD results.

Fan Operating Configuration	Run Nr.	Measured Airflow (m^3/s)[a]	Measured Mean Absolute Flow Angle (degrees)	CFD Model Mean Absolute Flow Angle (degrees)
Maximum (2 Fans, Sashes Open)	FA-4	14.94	1.8	1.8
Maximum (2 Fans, Sashes Open)	FA-5	14.75	2.6	
Minimum (2 Fans, Sashes Closed)	FA-6	10.92	2.9	2.2
Minimum (1 Fans, Sashes Closed)	FA-7	11.00	3.0	9.6

[a]Original data in scfm = standard cubic feet per minute; to convert 1 m^3/s = 2118.88 cfm.

Table 4. Gas-tracer comparison of measured data from HV-C2 tests (adapted from Table B.1 of Glissmeyer and Flaherty [2]) and CFD results.

Injection Port		Operating Fans	Test Port	Run Nr.	Measured % COV	Measured % Deviation from Mean	CFD Model % COV	CFD Model % Deviation from Mean
A	Center	A	3	GT-37	2.3	5.3	1.7	3.3
A	Center	A&B	3	GT-34	3.2	7.9	8.8	18.6
B	Center	B	3	GT-47	1.7	2.9	2.2	5.2
B	Center	A&B	3	GT-54	3.9	9.1	6.3	15.8

Table 5. Particle-tracer comparison of measured data from HV-C2 tests (adapted from Table B.2 of Glissmeyer and Flaherty [2]) and CFD results.

Injection Port	Operating Fans	Test Port	Run Nr.	Measured % COV	CFD Model % COV
A	A&B	3	PT-20	8.1	12.9
A	A	3	PT-14	3.7	18.7
B	B	3	PT-19	3.6	12.0

from testing of the HV-C2 test system, respectively. The CFD model gave consistently conservative particle uniformity results compared to the measured data. With the exception of one of the single fan cases, the CFD model tended to give

conservative tracer uniformity results compared to the measured data. The CFD model also gave higher COV values for velocity and flow angle for the one operating fan configuration. With two fans in operation, the results are very similar between the CFD predictions and measured results for velocity and flow angle. Overall, both the measured data and CFD predictions values are below the COV and variation limits specified in the ANSI/HPS N13.1-2021 standard.

This benchmarking exercise demonstrates the capability of the CFD modeling methodology to suitably simulate effluent stack operation and sampling location performance for a stack similar to that at the 3430 Building.

3. Stack Modeling Results

The CFD model simulating the updated ventilation system for the 3430 Building that includes three fans and an air blender was run to examine the mixing performance of the system when operating at design conditions. The simulation cases include one-, two-, and three-fan operations. The results of these runs are summarized in Table 6. Results flow angles ranging from 5.6˚ to 17.3˚, which is within the ANSI/HPS N13.1-2021 standard limit of 20˚. The velocity uniformity COV values range from 1.0% to 3.9%. Gas tracer COV values range from 0.3% to 5.2%, and particle tracer COV values range from 5.2% to 18.1%. All resulting COV values were below the limit of 20%, and in no case was the maximum gas tracer concentration deviation from the mean greater than 30%. Thus, the modeling results predict that flow angle, velocity, gas tracer, and particle tracer criteria established by the ANSI/HPS N13.1-2021 standard will be met for the updated 3430 Building three-fan exhaust system design.

Figure 5 shows a plan view of the velocity magnitude at the duct mid-plane (top) and resultant particle (bottom left) and tracer gas distributions (bottom right) at the sampling location for the 53.8-$m^3 \cdot s^{-1}$ (114,000-cfm) case running Fans 1, 2, and 3 with the injection point at the junction.

3.1. Stack Verification Testing

Stack verification tests were performed to collect velocity uniformity and flow angle measurements. Velocity uniformity tests were conducted with a standard pitot tube, a manometer to measure pressure, and a thermocouple to measure the temperature in the stack. The raw measurements collected by this method were in differential pressure units (inches of water). These measurements were converted to the velocity values needed to compute the velocity uniformity and estimate the mean velocity across the duct cross section.

The measurement procedure specified 10 measurement points across the diameter of the duct, and two duct traverses, 90 degrees apart, for a total of 20 discrete measurement positions. However, the ANSI/HPS N13.1-2021 standard prescribes that the points within the duct traverse that were within the center two-thirds of the stack area be used for the verification test calculations. A single test with three replicates of each of the two 90-degree separated traverses was conducted for this

stack verification measurement. The result of this test was a velocity uniformity of 2.1 %COV.

The measurement procedure used to collect cyclonic flow, or flow angle measurements, also specified 10 measurement points across the diameter of the duct.

Table 6. Summary of CFD modeling results for the three-Fan 3430 Building duct.

Operating Fan(s)	Injection Location	Flow per Fan [m³/s]	Total Flow [m³/s]	Velocity Uniformity % COV	Mean Absolute Flow Angle Degrees	Gas Tracer Uniformity		Particle Tracer Uniformity %COV
						% COV	% Deviation from Mean	
Fan1	Junction	5.38	5.38	2.7	8.8	2.3	3.2	15.3
Fan2	Junction	5.38	5.38	3.7	17.3	0.8	1.9	13.0
Fan3	Junction	5.38	5.38	2.9	7.4	0.8	1.7	9.2
Fan1	Junction	17.93	17.93	3.5	11.6	0.8	1.4	14.2
Fan2	Junction	17.93	17.93	2.4	15.7	0.3	2.4	10.2
Fan3	Junction	17.93	17.93	1.5	8.4	0.4	0.5	17.8
Fan 1, 2, & 3	Junction	5.38	16.14	2.1	8.2	3.2	4.9	16.9
Fan 1, 2, & 3	Junction	17.93	53.80	1.0	5.6	3.0	5.2	14.4
Fan 1 & 2	Junction	5.38	10.76	2.87	12.6	4.2	9.6	10.6
Fan 1 & 2	Junction	17.93	35.87	3.4	14.7	2.4	8.0	9.1
Fan 2 & 3	Junction	5.38	10.76	3.9	14.0	3.4	9.1	9.8
Fan 2 & 3	Junction	17.93	35.87	3.1	14.8	2.8	6.5	17.8
Fan 1 & 3	Junction	5.38	10.76	2.1	11.3	1.8	2.0	16.6
Fan 1 & 3	Junction	17.93	35.87	3.2	11.1	0.8	2.8	17.1
Fan 1	Fan 1	5.38	5.38	1.9	9.3	0.4	1.0	11.4
Fan 2	Fan 2	5.38	5.38	3.7	17.3	0.6	0.7	15.7
Fan 3	Fan 3	5.38	5.38	2.4	6.6	1.1	2.3	14.7
Fan 1	Fan 1	17.93	17.93	2.4	11.5	0.5	1.1	5.2
Fan 2	Fan 2	17.93	17.93	2.6	15.3	0.8	1.2	5.6
Fan 3	Fan 3	17.93	17.93	2.0	9.0	1.1	2.2	18.1
Fan 1, 2, & 3	Fan 2	5.38	16.14	2.2	9.9	5.2	7.2	7.1
Fan 1, 2, & 3	Fan 2	17.93	53.80	1.7	6.5	3.5	9.7	15.0
Fan 1 & 2	Fan 2	5.38	10.76	2.4	12.0	1.9	4.4	16.2
Fan 1 & 2	Fan 2	17.93	35.87	2.7	14.7	2.0	7.1	8.8
Fan 2 & 3	Fan 2	5.38	10.76	3.7	13.6	1.3	3.6	12.1
Fan 2 & 3	Fan 2	17.93	35.87	2.6	13.7	2.0	2.9	6.3
Fan 1 & 3	Fan 1	5.38	10.76	2.2	10.9	0.4	0.8	11.5
Fan 1 & 3	Fan 1	17.93	35.87	3.4	11.3	1.2	1.6	6.5

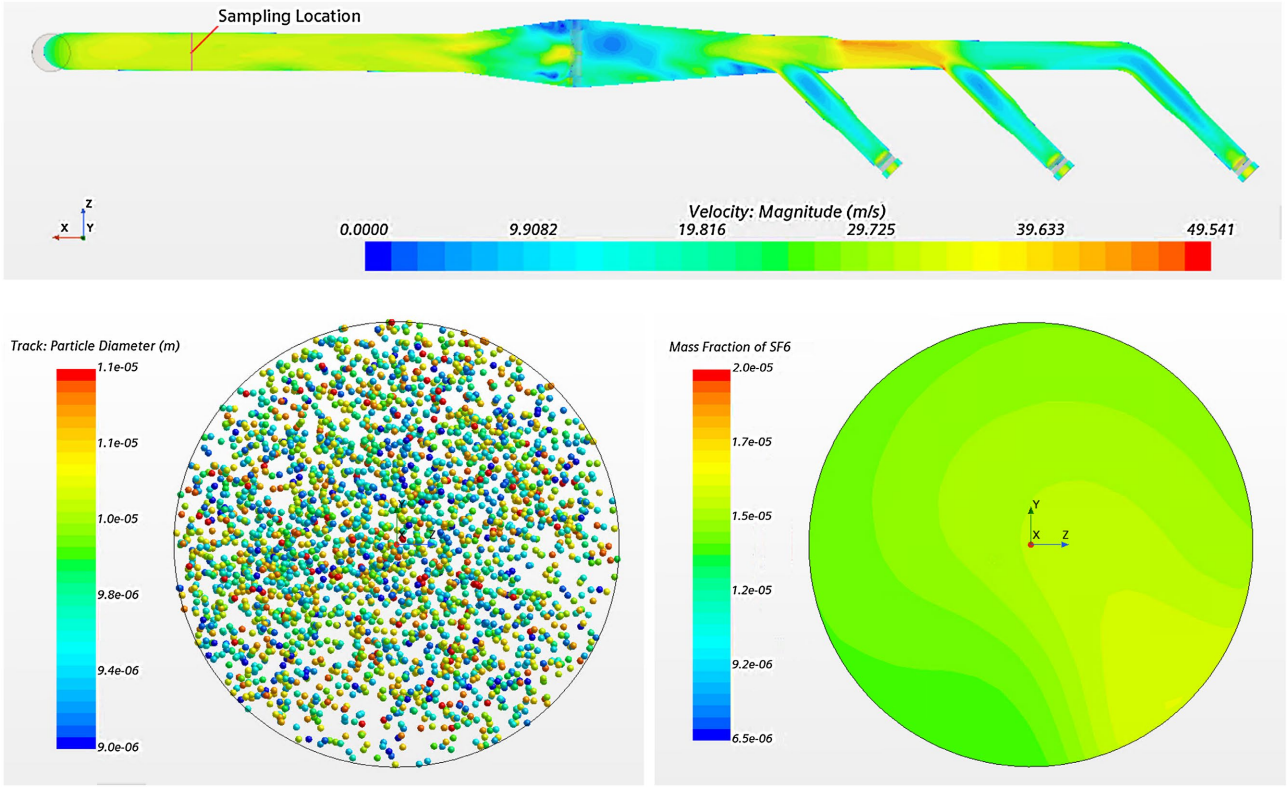

Figure 5. Plan view of velocity magnitude at mid-duct (top) and particle and tracer gas distributions at the sampling location (bottom left, right) for the 53.80 m^3/s (114,000-cfm) case operating Fans 1, 2, and 3 with the injection point at the junction.

Table 7. Velocity uniformity and flow angle results from the 3430 Building stack.

Operating Fans	Average Stack Flow Rate (m^3/s)	Flow Angle (degrees)	Velocity Uniformity (%COV)
2, 3	18.03	5.6	2.1

Due to equipment limitations, only a horizontal traverse was measured for this test, and only one traverse replicate was performed. In this instance, all 10 traverse points were used in the calculation of the mean flow angle across the duct. The result of this test was a mean flow angle of 5.6 degrees. The flow angle and velocity uniformity test results are summarized in Table 7.

3.2. CFD Model Comparisons with Verification Testing

Table 8 presents a subset of results from the CFD simulations that compares the results of velocity uniformity and flow angle from the CFD model to those measured during the 3430 Building stack verification tests. CFD model simulations incorporated two operating fans as well as three operating fans. The CFD simulations indicate that the stack sampling location had a slightly more uniform velocity, and slightly lower flow angle when three fans were operating, even if those three fans resulted in a lower flow rate, compared with two operating fans.

Broadly, then, the average velocity uniformity (%COV) results from the CFD

model were 2.74 %COV for a flow rate range from 5.38 to 53.80 m^3/s (11,400 to 114,000 cfm). Within a flow rate range from 10.76 to 30.39 m^3/s (22,800 to 64,400 cfm), the velocity uniformity was slightly higher at 2.85 %COV. The flow angle results varied from 5.6 - 17.3 degrees for all CFD cases, with an average flow angle of 11.3 degrees. The CFD results indicate that the velocity uniformity results and the flow angle results are relatively insensitive to stack flow or operating fan configuration, as the numerical results do not demonstrate a trend with flow or fan configuration, and the spread in the results are relatively small, particularly for the velocity uniformity (3 %COV; 12 degrees for flow angle).

Table 8. Velocity uniformity and flow angle results from the 3430 CFD model with both two and three fans in operation, and actual stack verification test results. CFD rows adapted from Suffield *et al.* [6].

Stack	Operating Fans	Stack Flow Rate (m^3/s)	Flow Angle (degrees)	Velocity Uniformity (%COV)
CFD	1, 2, 3	44.17	6.7	2.1
CFD	1, 2, 3	16.14	9.0	2.1
CFD	2, 3	29.45	13.4	3.8
CFD	2, 3	10.76	13.8	3.8
Actual	2, 3	18.03	5.6	2.1

The measured velocity uniformity verification test result was 2.1 %COV. This value is well within the uniformity criterion of ≤20% COV. Additionally, this value is well within the criterion that the actual stack measurement must be within 5% of the surrogate stack result of 2.74% COV for the CFD model.

Additionally, the measured average flow angle at the 3430 Building stack monitor location was 5.6 degrees. The CFD modeling predicted higher flow angles, indicating that the CFD model is conservative. Both the measured and CFD flow angles are ≤20 degrees, so the criterion is met.

The experimental uncertainty associated with the velocity uniformity result has several sources, which include instrument and data collection errors. Instrument errors are minimized by using calibrated equipment, and data collection errors are minimized through triplicate traverses to average the measurement position variance. Previous scale model and 2-fan tests at the 3430 facility included replicate tests at given stack fan and flow configurations to provide a measure of experimental uncertainty. In general, replicate test results indicate an experimental uncertainty of approximately 0.5 to 1.0% COV.

Model testing to determine numerical uncertainty has not been performed; however, the grid convergence described previously indicates that the uncertainty associated with the computational grid is less than 3% relative error. Given that the CFD results are relatively insensitive to flow rate, it is expected that the numerical uncertainty associated with the velocity uniformity results as likely on the order of 0.1% COV.

The estimated uncertainty for the experimental and numerical velocity uniformity results appear to be appropriate, as the difference of 1.7% COV is similar to the sum of the uncertainties (*i.e.*, 1.1% COV). This fits well with the requirement of the actual stack measurement to be within 5% COV of the surrogate stack.

Based on these stack verification test results, in conjunction with the CFD simulations, the reconfigured 3430 Building filtered exhaust stack meets the qualification criteria provided in the ANSI/HPS N13.1-2021 standard.

4. Summary

CFD modeling was used determine the final design modifications for the ventilation system for the 3430 Building radiological effluent stack. CFD modeling was used to gain insight into the expected performance of the modified stack and sampling location and to ensure that the new system would remain complaint with the ANSI/HPS N13.1-2021 standard. CFD model benchmarking showed that modeling results of flow angle, velocity uniformity COV, gas tracer uniformity COV, and particle-tracer uniformity COV values were in good agreement with those derived from testing of the original stack configuration with two fans and the physical tests of the HV-C2 physical test model used to help qualify the original 3430 Building stack. Modeling results of the modified ventilation system, which included a three-fan system with an air blender operating at the expected flow conditions, predict that flow angle, velocity uniformity, and tracer concentration criteria established by the ANSI/HPS N13.1-2021 standard will be met. The process of CFD modeling meets the intent of optimizing and upgrading a new or existing system as described in Section 6.9 of ANSI/HPS N13.1-2021.

This work continues to demonstrate the utility of CFD as a predictive tool for evaluating stack radioactive air emissions designs to the standards. With the use of CFD modeling the time (circa 10 weeks) and resources (greenhouse gas emissions, and particulate emissions) associated with physical scale model testing are abated, provided the CFD results are within 5% COV of the as-built velocity profile and the flow angle remains ≤ 20 degrees.

Acknowledgements

This work was conducted at the Pacific Northwest National Laboratory, which is operated for the U.S. Department of Energy by Battelle under Contract DE-AC0576RL01830.

Conflicts of Interest

The authors declare no conflicts of interest regarding the publication of this paper.

References

[1] Health Physics Society (2021) Sampling and Monitoring Releases of Airborne Radioactive Substances from the Stack and Ducts of Nuclear Facilities. ANSI/HPS N13.1-2021. Health Physics Society.

[2] Glissmeyer, J.A. and Flaherty, J.E. (2010) Assessment of the 3430 Building Filtered Exhaust Stack Sampling Probe Location. PNNL-19262, Revision 1. Pacific Northwest National Laboratory.

[3] Glissmeyer, J.A. and Droppo, J.G. (2007) Assessment of the HV-C2 Stack Sampling Probe Location. PNNL-16611. Pacific Northwest National Laboratory.

[4] Incropera, F.P. and DeWitt, D.P. (1985) Introduction to Heat Transfer. 2nd Edition, John Wiley and Sons.

[5] Barnett, J.M. and Snyder, S.F. (2021) Pacific Northwest National Laboratory Facility Radionuclide Emissions Points and Sampling Systems. PNNL-15992, Revision 5. Pacific Northwest National Laboratory. https://www.researchgate.net/publication/356909850_Pacific_Northwest_National_Laboratory_Facility_Radionuclide_Emission_Points_and_Sampling_Systems

[6] Suffield, S.R., Barnett, J.M. and Flaherty, J.E. (2023) Assessment of the 3430 Building Filtered Exhaust Stack Sampling Probe Location (Stack Verification Following Fan and Air Blender Additions), PNNL-35334. Pacific Northwest National Laboratory.

[7] Ballinger, M.Y., Recknagle, K.P. and Barnett, J.M. (2014) Comparison of a Computations Fluid Dynamics Model with Exhaust Flow Data from a Scale Model Stack. In: Barnett, J.M., Vazques, G.A., Bates, C.J. and Anderson, S.V., Eds., 2003 *Annual NESHAP Meeting on Radioactive Air*, Pacific Northwest National Laboratory, 50-67. https://www.researchgate.net/publication/292159232_2003_Annual_NESHAP_Meeting_on_Radioactive_Air

[8] Barnett, J.M., Ballinger, M.Y., Recknagle, K.P. and Yokuda, S.T. (2013) Computational Modeling of a Stack Sampling Location for Radioactive Air Emissions. In: Barnett, J.M., Vazques, G.A. and Bates, C.J., Eds., 2005 *Annual NESHAP Meeting on Radioactive Air*, Pacific Northwest National Laboratory, 73-84. https://www.researchgate.net/publication/292159045_2005_Annual_NESHAP_Meeting_on_Radioactive_Air

[9] Recknagle, K.P., Yokuda, S.T., Ballinger, M.Y. and Barnett, J.M. (2009) Scaled Tests and Modeling of Effluent Stack Sampling Location Mixing. *Health Physics*, **96**, 164-173. https://doi.org/10.1097/01.hp.0000333680.18803.8a

[10] Yu, X., Barnett, J.M., Amidan, B.G., Recknagle, K.P., Flaherty, J.E., Antonio, E.J., *et al.* (2018) Evaluation of Nitrous Oxide as a Substitute for Sulfur Hexafluoride to Reduce Global Warming Impacts of ANSI/HPS N13.1 Gaseous Uniformity Testing. *Atmospheric Environment*, **176**, 40-46. https://doi.org/10.1016/j.atmosenv.2017.12.015

[11] Siemens (2022) STAR-CCM+ User Guide, Version 17.06; Siemens Product Lifecycle Management Software, Inc.

[12] Barnett, J.M., Yu, X., Recknagle, K.P. and Glissmeyer, J.A. (2016) Modeling and Qualification of a Modified Emission Unit for Radioactive Air Emissions Stack Sampling Compliance. *Health Physics*, **111**, 432-441. https://doi.org/10.1097/hp.0000000000000557

[13] Barnett, J.M., Yu, X., Suffield, S.R. and Recknagle, K.P. (2020) Modeling Filtered Building Effluent Stack Sampling Points for Qualification Criteria. *Progress in Nuclear Energy*, **124**, Article ID: 103338. https://doi.org/10.1016/j.pnucene.2020.103338

[14] Ashraf, M.A., Hassan, A., Arif, Raza, A., Fatima, M. and Ullah, A. (2024) Identification of Exhaust Stack Sampling Location of a Research Reactor Considering ANSI/HPS N13.1-2011 Mixing Criteria Using Computational Fluid Dynamics. *Energy Sources, Part A: Recovery, Utilization, and Environmental Effects*, **46**, 3212-3227. https://doi.org/10.1080/15567036.2024.2314163

[15] Jensen, B.B.B. (2007) Numerical Study of Influence of Inlet Turbulence Parameters on Turbulence Intensity in the Flow Domain: Incompressible Flow in Pipe System. *Proceedings of the Institution of Mechanical Engineers*, *Part E*: *Journal of Process Mechanical Engineering*, **221**, 177-186. https://doi.org/10.1243/09544089jpme124

[16] Oberkampf, W.L. and Roy, C.J. (2010) Verification and Validation in Scientific Computing. Cambridge University Press. https://doi.org/10.1017/cbo9780511760396

[17] American National Standards Institute, Inc. (1970) Guide to Sampling Airborne Radioactive Materials in Nuclear Facilities. ANSI N13.1-1969. ANSI.